

Photoelectron energy-loss study of the $\text{Bi}_2\text{CaSr}_2\text{Cu}_2\text{O}_8$ superconductor

Z.-X. Shen, P. A. P. Lindberg, D. S. Dessau, I. Lindau, and W. E. Spicer
Stanford Electronics Laboratories, Stanford University, Stanford, California 94305-4090

D. B. Mitzi, I. Bozovic, and A. Kapitulnik
Department of Applied Physics, Stanford University, Stanford, California 94305-4090
(Received 26 October 1988)

Using energy-loss spectroscopy of photoelectrons from a single crystal of $\text{Bi}_2\text{CaSr}_2\text{Cu}_2\text{O}_8$, we show that the electronic structure of the near-surface region is consistent with that of the bulk. Utilizing the fact that photoelectrons of different elements are excited at different locations in the unit cell, we identify the energy-loss features as due to valence plasmon excitations, and one-electron excitations by comparing the photoelectron energy-loss spectra of the different elements.

Since the discovery of the high-temperature superconductors, electron-energy-loss spectroscopy (EELS) using high-energy primary electrons has been used to study the electronic structure of the superconductors.¹⁻⁴ In a typical EELS experiment, the electron-energy-loss features are caused by electrons that lose some of their energy by creating plasmon excitations or causing one-electron excitations, which could be either interband or intra-atomic transitions. Therefore, EELS spectra can provide information on the electronic structure of the material under study.

In this paper, we report an experimental observation of the energy-loss structures of x-ray emitted photoelectrons in x-ray photoemission spectroscopy (XPS) data from well-characterized single crystals of $\text{Bi}_2\text{CaSr}_2\text{Cu}_2\text{O}_8$. These energy-loss spectra of the photoelectrons, which have an escape depth of $\sim 25 \text{ \AA}$, show four prominent features which are consistent with the structures observed in a loss spectrum of electrons with a much higher primary energy of 170 keV, which have a probing depth of $\sim 1000 \text{ \AA}$.⁴ This indicates that the electronic structure of the $\text{Bi}_2\text{CaSr}_2\text{Cu}_2\text{O}_8$ compound, as revealed by EELS experiments, is very much the same in the bulk and in the near-surface region. This increases the credibility of previous experiments that utilized the surface-sensitive techniques such as photoemission.^{5,6} Moreover, further information can be gained by use of the fact that photoelectrons of the different elements originate from different parts of the unit cell.

Single crystals of $\text{Bi}_2\text{CaSr}_2\text{Cu}_2\text{O}_8$ were prepared by mixing powders of Bi_2O_3 , $\text{Sr}(\text{CO}_3)_2$, CaCO_3 , and CuO . X-ray-diffraction measurements showed an almost pure phase of $\text{Bi}_2\text{CaSr}_2\text{Cu}_2\text{O}_8$ in the crystals. The superconducting transition temperature T_c was determined by magnetic measurements to be 90 K. The samples were transferred into a Varian photoemission chamber through a fast-lock transfer system and then cleaved *in situ*. The orientations of the cleavage plane of the samples were determined by x-ray diffraction after the photoemission experiment.⁷ The base pressure of the chamber was 1×10^{-10} Torr. The surface area of the samples varied from 6 to 25 mm^2 . A Mg x-ray source (1253.6 eV) and a cylindrical mirror analyzer were used for the XPS mea-

surement with overall energy resolution of 1.2 eV. Because of the extremely weak signal of the photoelectron-energy-loss features, it took about 12 h to take one spectrum. Even though the data presented in this paper come from one single crystal, the same results were repeated for many of the samples we studied.

In order to characterize the single-crystal surface, we performed low-energy-electron-diffraction (LEED) experiments, which showed that the surface structure is consistent with the bulk structure.⁷ As we reported previously, our LEED patterns exhibit sharp, distinct spots without streaking, thus revealing a well-ordered single-crystalline surface.⁷ The LEED pattern can still be clearly seen after photoemission spectroscopy experiments even though the diffraction spots are somewhat fuzzier. This shows the stability of the sample surface in vacuum. The orientation of the cleavage plane was determined to be perpendicular to the c axis by x-ray diffraction⁷ and the terminating plane of the cleaved single-crystal surface was found to be the BiO plane.⁸

Figure 1(a) presents the O 1s core level which is a sharp single peak with a full width at half maximum (FWHM) of 2.5 eV. This implies that the binding energies of the O ions at the different O sites are very similar so that they cannot be resolved by 1.2-eV energy resolution. The structure marked S is due to a ghost line of the unmonochromatized x-ray source. There are weak structures extending up to 50-eV higher binding energy than that of the main core level which can be more clearly seen in the magnified spectrum. These structures arise from the O 1s photoelectrons that lose their energy during their traveling to the sample surface. In essence, this is the energy-loss spectrum of the O 1s photoelectrons. We can distinguish four prominent features in this spectrum, which are labeled $A1$, $B1$, $C1$, and $D1$. Their energies relative to the primary core line are also given in Fig. 1. Since the electrons traveling in the solid will lose their energy due to similar mechanisms, we expect to see loss spectra from the photoelectrons of the other core levels. Figure 1(b) presents the Bi 4f core level which is a sharp doublet without any indication of a second component, consistent with the fact that there is only one Bi site in the $\text{Bi}_2\text{CaSr}_2\text{Cu}_2\text{O}_8$ compound. The FWHM of the Bi 4f

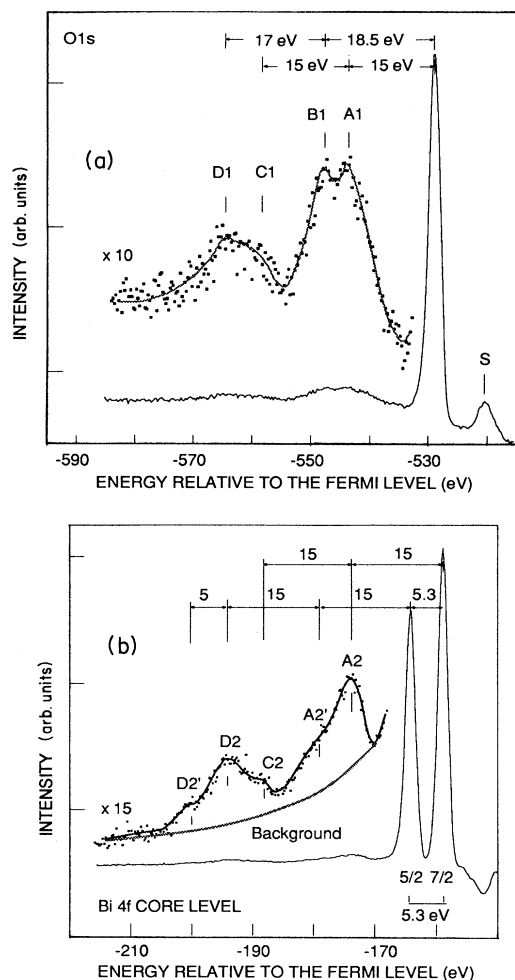


FIG. 1. (a) XPS spectrum of O $1s$ core level. The structure marked S is due to a ghost line of the x-ray source and the weak structures at higher binding energy are the energy-loss features of the O $1s$ photoelectrons. (b) XPS spectrum of Bi $4f$ core level. Again, the structures at higher binding energy are energy-loss features. In the magnified spectra, the points are experimental data and the solid lines are drawn to guide the eye.

peak is 1.9 eV and the spin-orbital splitting is 5.3 eV. Similar to the O $1s$ spectrum, there are weak structures extending up to 50-eV higher binding energy, which can be more clearly seen in the magnified spectrum. These structures arise from the Bi $4f$ photoelectrons that lose some of their energy before they leave the solid. The energy-loss spectrum of Bi $4f$ photoelectrons is more complicated since it is created by doublet primary peaks. Five prominent features are observed in the spectrum which are marked as $A2$, $A2'$, $C2$, $D2$, and $D2'$.

In order to understand the origin of these structures, we plot in Fig. 2 both spectra of Fig. 1, shifted so that the O $1s$ and the Bi $4f_{7/2}$ peaks are matched. The energies of the other features are given relative to the main lines. It is clear that the features $A2$, $C2$, and $D2$ are at the same energies as the features $A1$, $C1$, and $D1$, respectively,

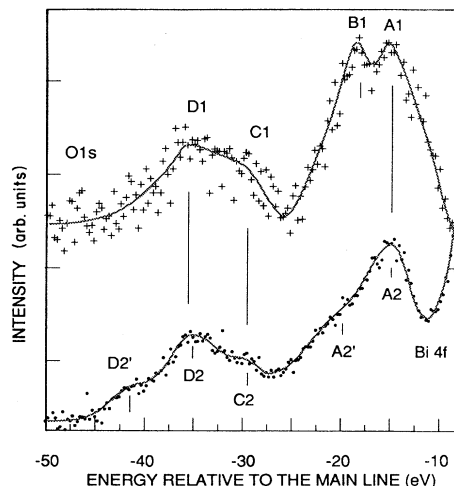


FIG. 2. The energy-loss spectra of O $1s$ and Bi $4f$ photoelectrons plotted relative to the primary core level. The O $1s$ and Bi $4f_{7/2}$ core levels are matched.

which makes it conceivable that they are caused by the same energy-loss mechanisms. Bearing in mind that the Bi $4f$ core level is a doublet with a spin-orbital splitting of 5.3 eV, one expects that the energy-loss spectrum of the Bi $4f$ photoelectrons is a superposition of two sets of energy-loss structures of single primary peaks separated in energy by 5.3 eV. Because the energy separation of feature $A2'$ ($D2'$) and $A2$ ($D2$) also is ~ 5 eV, we conclude that features $A2'$ and $D2'$ are of the same energy-loss origin as features $A2$ and $D2$, respectively. This figure shows that feature B , which is very prominent in the energy-loss spectrum of the O $1s$ photoelectrons, is not observed or is much weaker in the energy-loss spectrum of Bi $4f$ photoelectrons. It should be pointed out that the intensity ratio of features $A2'$ and $A2$ is not the same as the intensity ratio of the two spin-orbital components of the Bi $4f$ core level. The reason for this remains unclear. However, this will not affect our main conclusion that feature B is not observed in the Bi spectrum. It should also be noted that an EELS experiment using high-energy electrons, which has a probing depth of 1000 Å, yields similar energy-loss spectra with prominent features located at the same energies as the features A , B , C , and D .⁴

Summarizing our experimental data, we see four energy-loss features A , B , C , and D in the loss spectrum of the O $1s$ photoelectrons, but feature B is not observed in the energy-loss spectrum of the Bi $4f$ photoelectrons. In Fig. 3 we sketch our schematic interpretation of the photoemission process from the $\text{Bi}_2\text{CaSr}_2\text{Cu}_2\text{O}_8$ compound. Since the unit cell of the superconductor is very large and the cleavage plane is the BiO plane, the Bi $4f$ photoelectrons originate mainly from the first layer in the crystal, because of the short probing depth and the fact that the second BiO layer will be ~ 15 Å deeper in the crystal. (Note that the escape depth of the Bi photoelectrons is about 25 Å.) Therefore, Bi $4f$ photoelectrons are mainly created in the top layer so that the loss features A , C , and D , which are observed in the energy-loss spectrum of Bi $4f$

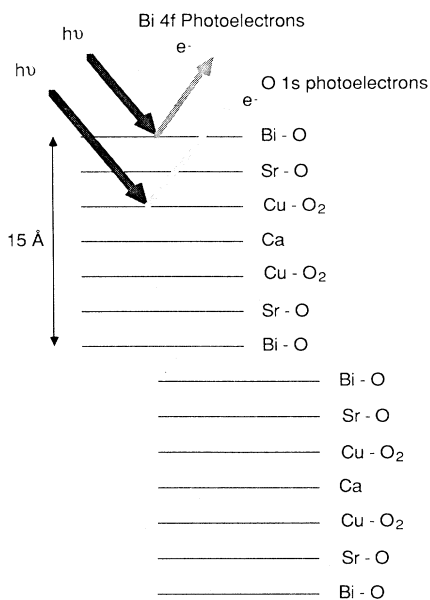


FIG. 3. Sketch of the photoemission from $\text{Bi}_2\text{CaSr}_2\text{Cu}_2\text{O}_8$ compound, with the BiO plane terminating the single crystal.

photoelectrons, are associated with one or perhaps two top atomic layers (i.e., the BiO and SrO planes as shown in Fig. 3). On the other hand, feature *B*, which is not observed in the loss spectrum of the Bi 4*f* photoelectrons but appears prominently in the loss spectrum of the O 1*s* photoelectrons, is clearly not associated with the surface layer.

The assignment of the energy-loss features is not a trivial task. The main channels through which the primary electrons lose their energies are plasmon excitations or one-electron excitations. The cross section for creation of volume plasmons is usually high so that the peak of the loss function $\text{Im}(-1/\epsilon)$ usually corresponds to the volume-plasmon frequency.^{2,3} In the case of $\text{YBa}_2\text{Cu}_3\text{O}_7$, the maximum of the loss spectrum at 25 eV is assigned to volume plasmons.^{2,3} To help identify the one-electron excitations, we list in Table I the relevant energy levels of the elements involved. Based on Table I and the energies of features *A*, *B*, *C*, and *D*, we find that the following transitions are the possible candidates for the prominent energy-loss features observed: Bi 5*d* → Bi 6*p*, Bi 6*s* → Bi 6*p*, Sr 4*p* → Sr 4*d*, Ca 3*p* → Ca 3*d*, O 2*s* → O 2*p*.

Let us first look at feature *B*1 at 18.5 eV, which, as we pointed out earlier, is not associated with the top BiO plane. We tentatively assign this feature to the volume partial valence plasmon excitation. [If Cu 3*d*, O 2*p*, and Bi 6*s* electrons are assumed to contribute to the electron density N , a crude estimate with $m = m_e$ and $\epsilon(\infty) = 1$ gives $\hbar\Omega_p = \hbar(4\pi Ne^2/m)^{1/2} = 21$ eV.] This assignment can naturally explain the fact that feature *B* cannot be seen in the energy-loss spectrum of the Bi 4*f* photoelectrons which are created in the top atomic layer. In this way, using the fact that the photoelectrons originate from different parts of the crystal, we gain information which cannot be obtained by EELS experiments with very high

TABLE I. Energy levels of different elements in the high- T_c compound in eV with respect to E_F . Here we do not list the Cu 3*d*-O 2*p* states in the valence and the conduction band. The asterisk means uncertain experimental values.

States	Energy levels (eV)
Bi 5 <i>d</i>	-28.5, -25.5 ^a
Bi 6 <i>s</i>	-11 ^b , -13 ^c
Bi 6 <i>p</i>	4-5 ^d (centroid)
Bi 6 <i>d</i>	above 25 ^d
O 2 <i>s</i>	-18 ^{*c}
Sr 4 <i>p</i>	-18.5 ^a
Sr 4 <i>d</i>	12.6 ^d
Ca 3 <i>p</i>	~ -24 ^{*d}
Ca 3 <i>d</i>	8.5 ^d

^aReference 9.

^bReference 10(a).

^cReference 10(b).

^dReference 11.

^eReference 12.

primary beam energies.⁴ It should be pointed out here, however, that Takahashi *et al.* reported that the O 2*s* level has a binding energy of 18 eV (as listed in Table I), and, therefore, it would be possible for the O 2*s* → O 2*p* transition to occur around 18-19 eV. We consider this less likely since the 18.5-eV feature is not seen in the energy-loss spectrum of the Bi 4*f* photoelectrons. For otherwise the Bi 4*f* photoelectrons would be able to induce this transition in the oxygen atoms in the top BiO plane, since the acceptance angle of our experimental setup is very large.

As we pointed out earlier, features *A*, *C*, and *D* are associated with the BiO and SrO planes. There are two possibilities for the origin of feature *A*: (a) It may be due to the Bi 6*s* → Bi 6*p* transition, which, according to Table I, has an energy around ~ (15-18) eV. (b) It may be due to surface plasmon excitations. We prefer the second possibility since Wagener *et al.* also have observed a 15-eV plasmon feature in their inverse photoemission data.¹¹ Feature *C* (~30 eV) may be the Sr 4*p* → Sr 4*d* transition because the transition threshold energy is about 30 eV. However, because of the so-called giant dipole resonance process, the maximum in excitation cross section could occur 10-15 eV above the one-electron threshold.¹¹ Therefore, one should be cautious about this assignment. The other possible origin of feature *C* is a double plasmon loss. The argument against this is that its intensity is too strong, for the intensity ratio of feature *C* and feature *A* is much larger than the intensity ratio of feature *A* and the primary peak. Feature *D* (~35 eV) is tentatively assigned to the Bi 5*d* → Bi 6*p*-O 2*p* transitions.

In summary, we report the experimental observation of the energy-loss structures in the core-level XPS data from well-characterized single-crystalline surfaces of $\text{Bi}_2\text{CaSr}_2\text{Cu}_2\text{O}_8$, which we interpret as the results of one-electron excitations and valence plasmon excitations. The prominent features observed in the energy-loss spectra of the photoelectrons are the same as those obtained from the electron-loss spectra of high-energy primary electrons,

demonstrating that the information obtained from within 25 Å of the surface is consistent with that obtained from the bulk. Furthermore, because the photoelectrons of different elements are excited in different parts of the unit cell, we are able to identify the origins of the energy-loss features by comparing the energy-loss spectrum of the different elements.

We would like to thank B. O. Wells for his help in our experiments. One of us (Z.-X.S.) wants to thank Professor C. Herring, Professor W. A. Harrison, Professor A.

Fetter, and Professor J. Weaver of University of Minnesota for many stimulating discussions. D.S.D and A.K. would like to acknowledge the support received from National Science Foundation and D.B.M. acknowledges support from AT&T. This work is supported by the U.S. National Science Foundation through the NSF-MRL program at the Center for Material Research at Stanford University, Air Force Contracts No. AFOSR-87-0389 and No. F49620-88-K0002 and Joint Services Electronics Program Contracts No. DAAG29-85-K-0048 and No. N00014-84-K-0327.

-
- ¹Y. Chang, M. Onellion, D. W. Niles, R. Joynt, G. Margaritondo, N. G. Stoffel, and J. M. Tarascon, *Solid State Commun.* **63**, 717 (1987).
- ²C. H. Chen, L. F. Schneemeyer, S. H. Liou, M. Hong, J. Kwo, H. S. Chen, and J. V. Waszczak (unpublished).
- ³C. Tarrío and S. E. Schnatterly, *Phys. Rev. B* **38**, 921 (1988).
- ⁴J. Fink, N. Nücker, H. Romerg, and S. Nakai, *Proceedings of the International Symposium on the Electronic Structure of High Temperature Superconductors*, Rome, 1988 (unpublished).
- ⁵Z.-X. Shen, P. A. P. Lindberg, I. Lindau, W. E. Spicer, C. B. Eom, and T. H. Geballe, *Phys. Rev. B* **38**, 7152 (1988); Z.-X. Shen, P. A. P. Lindberg, B. O. Wells, D. B. Mitzi, I. Lindau, W. E. Spicer, and A. Kapitulnik, *Phys. Rev. B* **38**, 11820 (1988).
- ⁶M. Onellion, M. Tang, Y. Chang, G. Margaritondo, J. M. Tarascon, P. A. Morris, W. A. Bonner, and N. G. Stoffel, *Phys. Rev. B* **38**, 881 (1988).
- ⁷P. A. P. Lindberg, Z.-X. Shen, B. O. Wells, D. B. Mitzi, I. Lindau, W. E. Spicer, and A. Kapitulnik, *Appl. Phys. Lett.* **53**, 2563 (1988).
- ⁸P. A. P. Lindberg, Z.-X. Shen, B. O. Wells, D. S. Dessau, D. B. Mitzi, I. Lindau, W. E. Spicer, and A. Kapitulnik, *Phys. Rev. B* **39**, 2890 (1989).
- ⁹P. A. P. Lindberg, P. Soukiassian, Z.-X. Shen, C. B. Eom, I. Lindau, W. E. Spicer, and T. H. Geballe, *Appl. Phys. Lett.* **53**, 1970 (1988).
- ¹⁰(a) Mark S. Hybertsen and L. F. Mattheiss, *Phys. Rev. Lett.* **60**, 1661 (1988); (b) F. Herman, R. V. Kasowski, and W. Y. Hsu, *Phys. Rev. B* **38**, 204 (1988).
- ¹¹T. J. Wagener, Yongjin Hu, Y. Gao, M. B. Jost, J. H. Weaver, N. D. Spencer, and K. C. Goretta, *Phys. Rev. B* **39**, 2928 (1989); and J. H. Weaver (private communication).
- ¹²T. Takahashi, H. Matsuyama, H. Katayama-Yoshida, Y. Okabe, S. Hosoya, K. Seki, H. Fujimoto, M. Sato, and H. Inokushi, *Nature (London)* **334**, 691 (1988).